Developmental Biology 454 (2019) 29–43

Contents lists available at ScienceDirect

Developmental Biology

journal homepage: www.elsevier.com/locate/developmentalbiology

Morphological characteristic and functional dependencies of dendritic cell in developing rabbit lung during fetal and neonatal life

Doaa M. Mokhtar *, Marwa M. Hussein

Department of Anatomy and Histology, Faculty of Veterinary Medicine, Assiut University, Assiut, 71526, Egypt

ARTICLE INFO

Keywords:
CD8
Ultrastructure
Telocytes
CD34
Lymphocytes
Antigen-presentation

ABSTRACT

Recently, pulmonary DC deserved the attention of researchers and clinicians as it was implicated in many diseases afflicting human lungs. However, there are no available data about the morphological or functional features of pulmonary dendritic cells in fetal or early neonatal life. The present study aimed to demonstrate the morphological development of DCs using light-, electron-microscopy, and immunohistochemistry. DCs showed strong immunoreactivity for both CD8 and CD56. Moreover, DCs strongly expressed CD34, VEGF, NSE, and connexin-43 within the developing pulmonary tissue. By SEM, DCs were polyhedral in shape with short cell processes in fetal life. By the advancement of the age, DCs became more numerous and exhibited rounded to oval cell bodies with many fine dendrites. TEM revealed that at early fetal life, DCs were characterized by their heterochromatic indented nuclei, few cell processes and few organelles. With the advancement of age, DCs showed dendrite-like processes and displayed signs of high endocytic activities with releasing of secretory materials. At late fetal life, DCs showed an obvious increase in the nuclear/cytoplasmic ratio and they exhibited a unique connection with type II pneumocytes and pulmonary endothelium by gap junction. In the early neonate, the DCs cells were seen in association with T-lymphocytes, neutrophils, telocytes (TCs), and air-blood barrier. They possessed many fine dendrites, the characteristic Birbeck granules and many vesicles. DCs may contribute to apoptosis, endocytosis, and angiogenesis. The difference in the maturation status may reflect different roles for DCs in the lung. The immature DCs may have an antigen-uptake role through endocytosis, while mature DCs may involve in antigen presentation to T-cells.

1. Introduction

Dendritic cells (DCs) are specialized highly professional antigen-presenting cells (APC) that are located at sites of the body where maximal microbial encounter occurs, such as the skin, the lung and the gut (Merad et al., 2013). DCs play a central role in the initiation of adaptive immune responses against foreign agents, infective agents, commensals or tissue damage.

In the last few years, pulmonary dendritic cells have been implicated in a number of pathologies afflicting human lungs such as bronchial asthma (Lambrecht and Hammad, 2003) and chronic obstructive pulmonary disease (COPD) (D'Hulst et al., 2002). Moreover, pulmonary dendritic cells have been shown to be the key cells in the protection against pulmonary tuberculosis infection in mice (Demangel et al., 1999; Lagranderie et al., 2003). Furthermore, recent studies showed that the number of pulmonary DCs is markedly increased in sarcoidosis (Buczkowski et al., 2002), in diffuse panbronchiolitis (Todate et al., 2000) and in lung cancer in humans (Hansen and Andersen, 2017). These findings have pushed many researchers to investigate and study the pulmonary DCs carefully in humans and in experimental animals. Hopefully, a better understanding of the morphological and physiological features of pulmonary DCs will provide new insights into the pathogenesis of those diseases, and will guide the clinicians to the design of new therapeutic strategies in control and prevention of these diseases by utilizing the unique properties of these cells.

In general, there are two major subsets of DCs, namely, myeloid DCs (mDCs) and plasmacytoid DCs (pDCs) (Shortman and Liu, 2002; Liu, 2005; Liu, 2001). Recently both subsets were recognized in the lungs of adult humans and mice (Shortman and Liu, 2002). On a functional level, mDCs include a heterogeneous population of antigen-presenting cells that have the capacity for the capture, processing, and presentation of antigens to T cells. Simply, mDCs act as a bridge linking between adaptive and innate immune responses. In the other hand, pDCs play a critical role in anti-viral immunogenic response and recently, it was proven that

* Corresponding author.
E-mail addresses: doaamokhtar33@yahoo.com, doaa@aun.edu.eg (D.M. Mokhtar).

https://doi.org/10.1016/j.ydbio.2019.06.013
Received 2 April 2019; Received in revised form 10 June 2019; Accepted 19 June 2019
Available online 21 June 2019

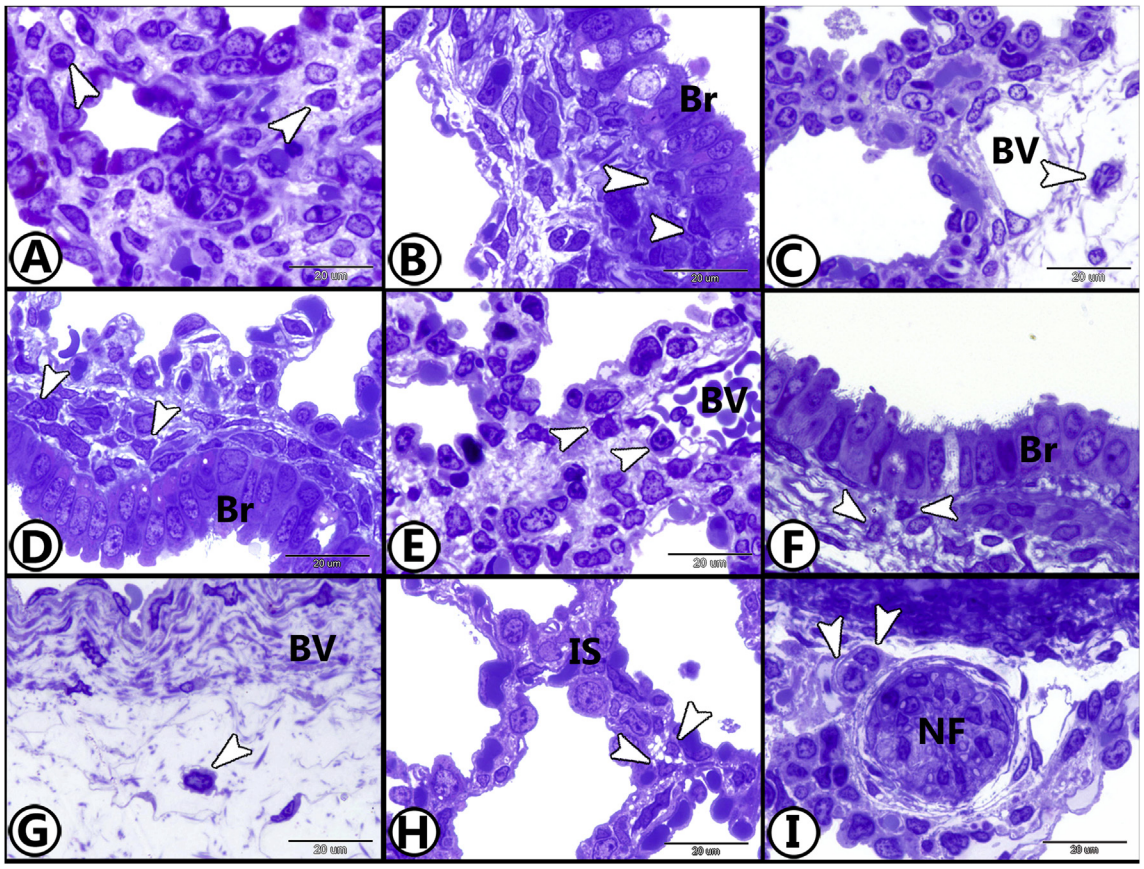

Fig. 1. Semithin section stained with toluidine blue in fetal and neonate rabbit lung.
A: in 25th gestational day, DCs (arrowheads) were recognized in pulmonary interstitial tissue. B-C: in 27th gestational day, DCs (arrowheads) were recognized in lamina propria of bronchiole (Br) and in tunica adventitia of developing blood vessels (BV). **D-E:** in 29th gestational day, DCs (arrowheads) were demonstrated in lamina propria of bronchiolar mucosa (Br) and in the wall of growing blood vessels (BV) beneath the endothelial cells. **F-I:** in 7th postnatal day, DCs (arrowheads) were demonstrated in lamina propria of bronchioles (Br), in adventitia of blood vessels (BV), in interalveolar septa (IS) and around nerve fibers (NF).

pDCs have also a clear very important tolerogenic role (McGovern et al., 2014).

Recent studies have shown that DC precursors and monocytes separate in the bone marrow. DC precursor gives rise to pre-DCs, which leave the bone marrow to reach the different organs and tissues, pre-DCs differentiate into several different subsets of DCs including $CD8^+DEC205^+$ and $CD8^+33D1^+$ in the spleen and $CD103^+$ and $CD8^+$ DCs in non-lymphoid tissues (Liu and Nussenzweig, 2010). Moreover, $CD8^+$ DCs have been considered as independent DC subpopulations both ontogenetically and functionally so that the wide variety of DC subsets can be classified on the basis of their CD8 expression (Banchereau et al., 2000).

DCs show a distinct set of cell-surface markers (Shortman and Liu, 2002 and Dudziak et al., 2007), which is used extensively in their identification and characterization. However, there is no single cell-surface antigen that identifies all DCs (Shortman and Liu, 2002). This is partially due to the fact that DCs are a heterogeneous group of cells that contain several distinct subpopulations (Liu, 2005 and Liu, 2001). The heterogeneity among DCs is of interest as it indicates specialized functional properties of each DCs subset. However, this heterogeneity also represents a strong challenge during recognizing of the DCs in different tissues and determining how these cells differ developmentally from other mononuclear cells, such as monocytes and macrophages. For these reasons, it was found that the ultra-structural approach is the best method to identify and count the total DCs population in pulmonary tissue and other organs (Shamoto et al., 1999; Teunissen, 1992).

Although the characteristics of pulmonary DCs have been extensively studied in many experimental animal models, only limited insufficient data are available concerning the rabbit pulmonary DCs (Koshy et al., 2003). Moreover, there are no available data at all about the morphological or functional features of pulmonary dendritic cells in fetal life. So that the aim of this study is to describe the morphological development of the dendritic cells in the rabbit lung and identify their populations using immunohistochemistry, morphometry, and electron microscopy.

2. Materials and methods

2.1. Collection of samples

The study was approved by the Ethics Committee of Assiut University, Egypt. Twenty-four New Zealand White rabbit fetuses collected on gestational days; 23, 25, 27 and 29 days (six fetuses per age) were used in the present study. In addition, six newborn New Zealand White rabbits were sacrificed on the 7th day of the postnatal period. The animals were obtained from the laboratory animals' house at Faculty of Medicine, Assiut University. Before the sacrifice of pregnant rabbit doe, the animals were anesthetized by 35 mg/kg ketamine and 5 mg/kg xylazine (Thurmon et al., 1996), and then the uterus was extracted. The fetuses were immediately taken out from the uterus and washed with normal saline. The obtained fetuses were prevented from breathing by tying their necks

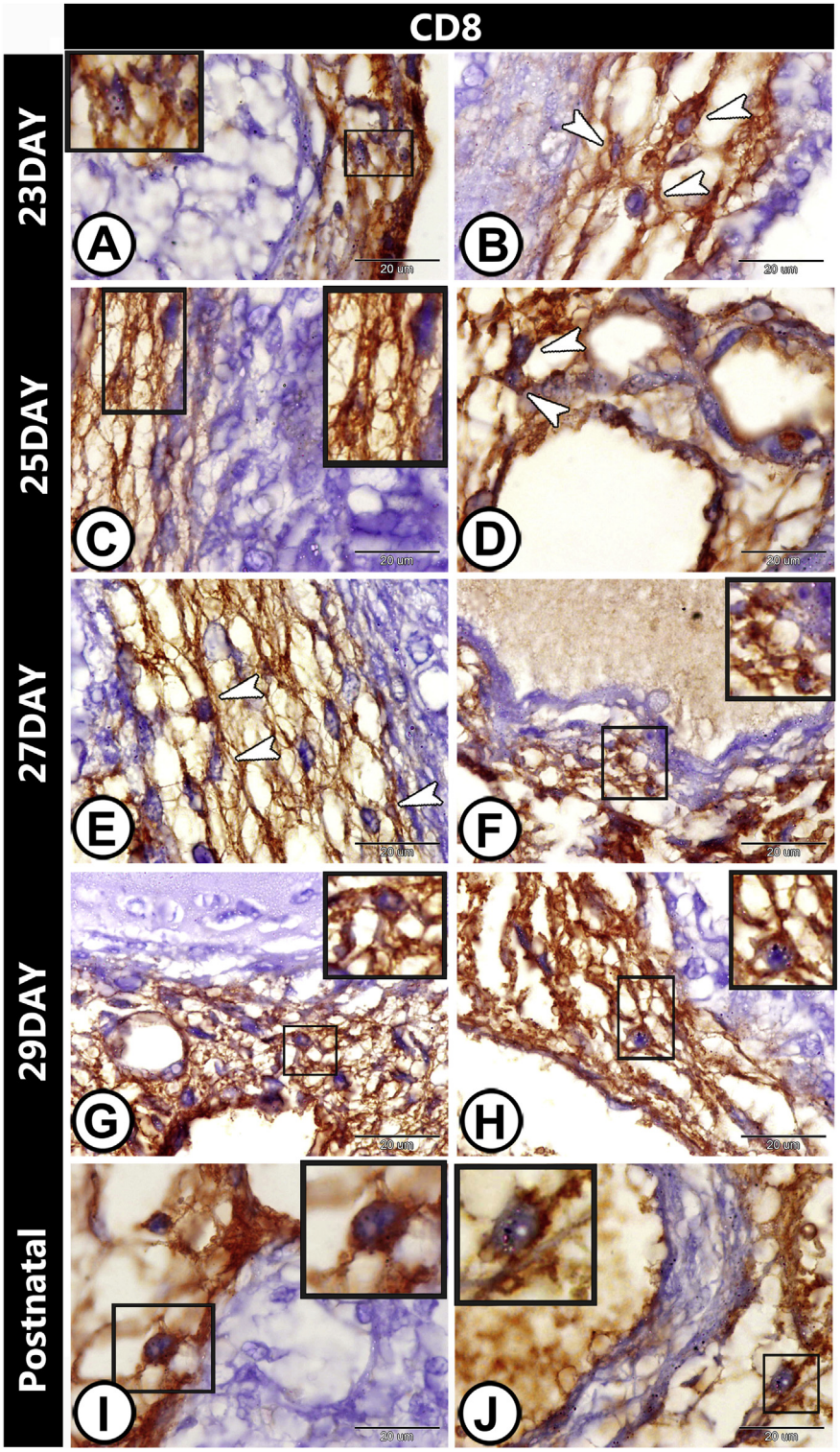

Fig. 2. Immunohistochemical expression pattern of CD8 in lungs at different developmental ages.
A: $CD8^+$ DCs (inserted figure) were recognized around nerve fibers (NF). **B:** $CD8^+$ DCs (arrowheads) were observed within bronchiolar mucosa (Br). **C-D:** $CD8^+$ DCs (inserted figure and arrowheads) were demonstrated in bronchiolar mucosa (Br) and in pulmonary interstitial tissue in close association with developing blood vessel (BV). **E-F:** $CD8^+$ DCs (inserted figure and arrowheads) were recognized in pulmonary interstitial tissue and in the wall of developing blood vessels (BV). **G-H:** $CD8^+$ DCs (inserted figure) were demonstrated in bronchial mucosa around cartilage plates (C) and in tunica adventitia of blood vessel (BV). **I-J:** $CD8^+$ DCs (inserted figure) were recognized in pulmonary interstitial tissue and in the tunica adventitia of developing blood vessels (BV).

after their extraction. All sacrificed animals and collected fetuses were dissected under a Stereo microscope, and both lungs were carefully excised immediately for fixation.

2.2. Immunohistochemistry

The immunohistochemistry was performed on formalin-fixed, paraffin-embedded, and 3-μm-thick step-serial sections were made from the lung samples collected at the five ages. The sections were treated with 10 ml Mol Tris buffer and 1 ml Mol ethylene-diamine-tetra-acetic acid, pH 9.0 for 20 min at 90 °C. Inhibition of endogenous peroxidase was done by soaking the sections with 3% H2O2, then they were preincubated overnight at 4 °C in 1% bovine serum albumin in PBS. The sections were stained at room temperature for 30 min, using the

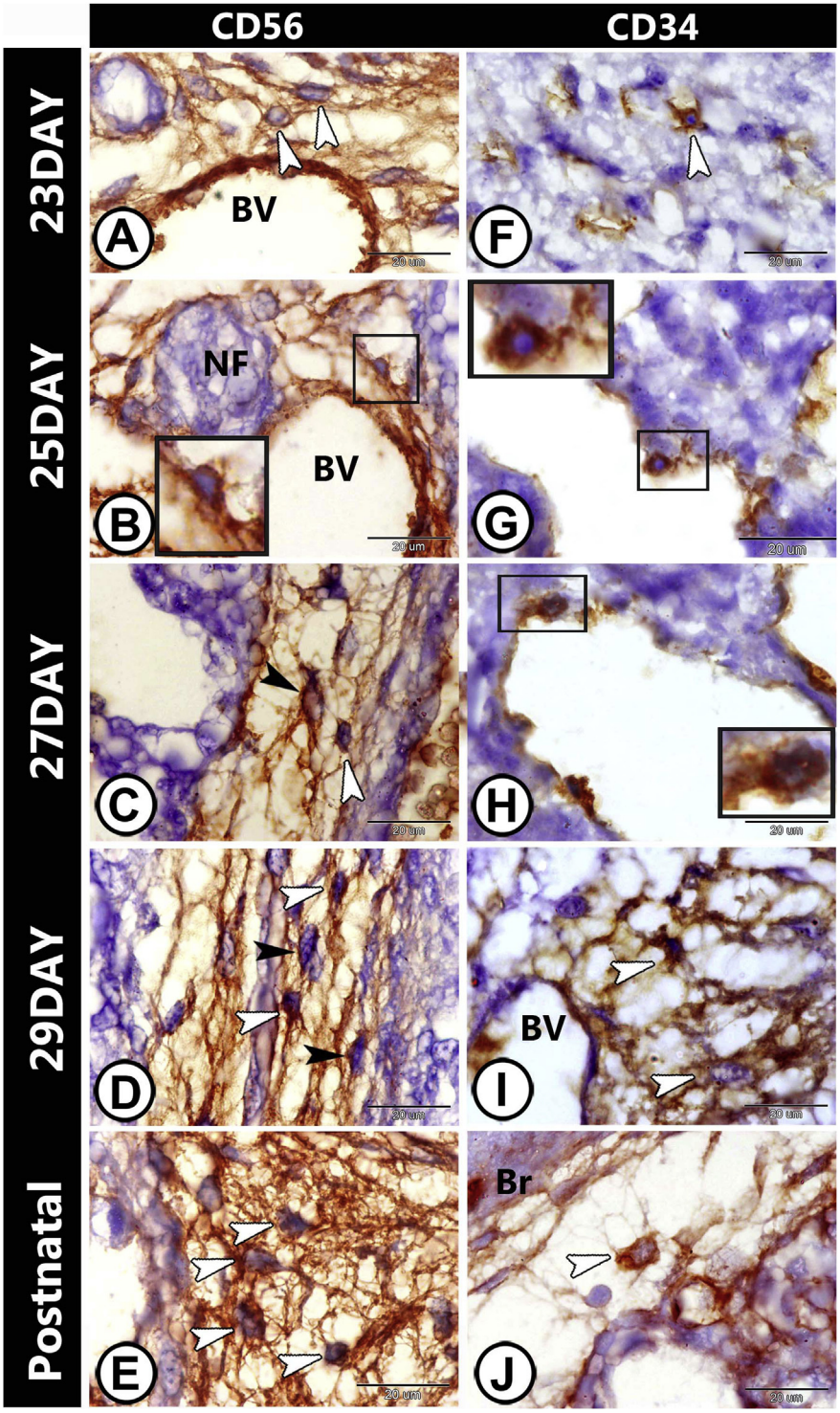

Fig. 3. Immunohistochemical expression pattern of CD 56 and CD 34 in lungs at different developmental ages. A: $CD56^{+}$ DCs (arrowheads) were observed in pulmonary interstitial tissue in close association with developing blood vessels (BV). **B:** $CD56^{+}$ DCs (inserted figure) were observed in pulmonary interstitial tissue in close association with developing blood vessels (BV) and nerve fiber (NF). **C-E:** $CD56^{+}$ DCs (white arrowheads) were demonstrated within the pulmonary interstitial tissue contacted to each other and to TCs (black arrowheads) by their cytoplasmic processes forming a network. **F:** CD 34^{+} DCs (arrowhead) were recognized in pulmonary interstitial tissue. **G:** $CD34^{+}$ DCs (inserted figure) were within the wall of developing airway and protruded to the lumen. **H:** CD 34^{+} DCs (inserted figure) were seen within the wall of developing blood vessel protruding to the vascular lumen. **I-J:** $CD34^{+}$ DCs (arrowheads) were observed in pulmonary interstitium surrounding blood vessels (BV) and developing bronchioles (Br).

following antibodies: rabbit polyclonal anti-vascular endothelial growth factor (VEGF) (1:300; Abcam, Cambridge, UK), rabbit polyclonal anti-NSE (neuron-specific enolase) (1:50, Dako, Glostrup, Denmark), mouse monoclonal anti-CD34 (1:100, clone QBEND10, Biogenex, San Ramon, CA, USA), mouse polyclonal anti-CD8 (1:200; Abcam, Cambridge, UK), mouse polyclonal anti-CD56 (1:200; Abcam, Cambridge, UK), and rabbit polyclonal anti-connexin 43 (1:400 Dako, Glostrup, Denmark) according to the avidin–biotin peroxidase complex method, as previously reported (Hsu et al., 1981). Sections were counterstained with hematoxylin and photographed under a Leica microscope (Germany).

2.3. Semithin and transmission electron microscopy

Small fragments of lung tissue in all ages were fixed in 2.5% paraformaldehyde and 2.5% glutaraldehyde in 0.1M sodium cacodylate buffer, pH 7.3 and left overnight at 4 °C (Karnovsky, 1965). Then

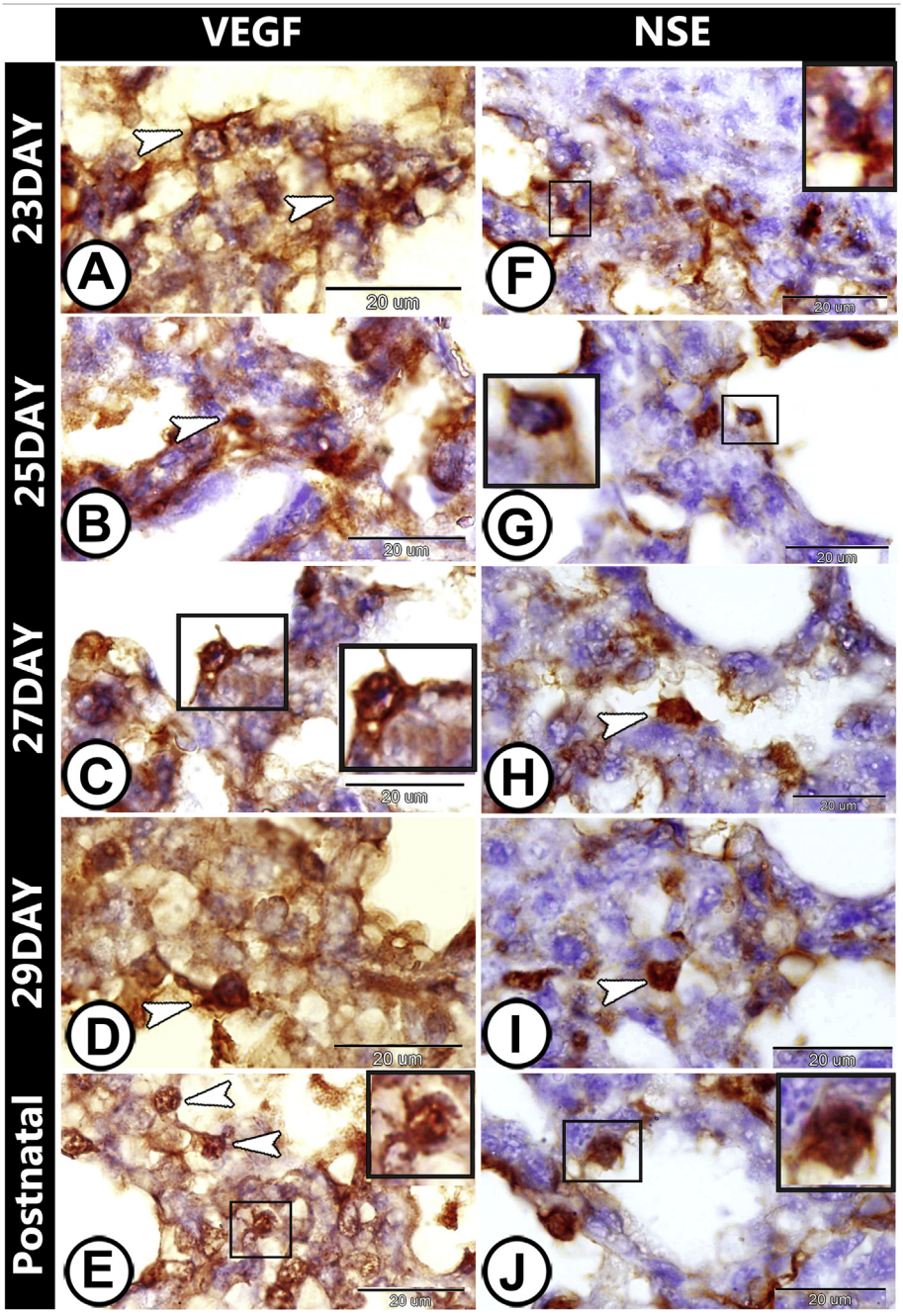

Fig. 4. Immunohistochemical expression pattern of VEGF and NSE in lung at different developmental ages.
A-B: DCs (arrowheads) expressed a strong VEGF immunoreactivity in pulmonary interstitial tissue **C:** DCs (inserted figure) expressed a strong VEGF immunoreactivity within inter-saccular septa. Note that its cytoplasmic processes are protruding to the airway lumen. **D-E:** DCs (arrowheads and inserted figure) expressed a strong VEGF immunoreactivity in close vicinity to the developing blood vessels (BV). **F:** DCs (inserted figure) expressed a strong NSE immunoreactivity in pulmonary interstitium. **G-H:** DCs (inserted figure and arrowheads) expressed a strong NSE within the wall of developing airways. **I-J:** DCs (arrowhead and inserted figure) expressed a strong NSE in pulmonary interstitium (IS) and within the wall developing alveoli (AL).

post-fixed in 1% osmic acid in 0.1M Na-cacodylate buffer for 2 hours at room temperature. The samples were then dehydrated in ethanol and embedded in Araldite-Epon mixture. Semithin sections (1 μm in thickness) were cut and stained with Toluidine blue and examined under a light microscope. Ultrathin sections were stained with uranyl acetate and lead citrate (Reynolds, 1963) and photographed under a JEOL 100 II transmission electron microscope.

2.4. Scanning electron microscopy (SEM)

Small specimens from the lung at the all studied ages were washed in 0.1M sodium phosphate buffer and fixed in 2.5% paraformaldehyde and 5% glutaraldehyde in 0.1M sodium phosphate buffer, pH 7.3, at 4 °C for 24 h. Then, they were post-fixed in 1% osmic acid in 0.1M sodium phosphate buffer for 2 h, dehydrated by acetone and then were subjected to critical-point drying with a Polaron apparatus. Finally, they were coated with gold using the JEOL- 1100 E ion-sputtering device and examined with a JEOL scanning electron microscope (JSM 5400 LV) at 10 kV.

2.5. Morphometrical and statistical analysis

2.5.1. Detection of age-related change in the number of DCs/unit area

Five immuno-stained sections were randomly selected from three immunohisochemical markers at each developmental age and five microscopic fields were randomly selected and analyzed using image-J

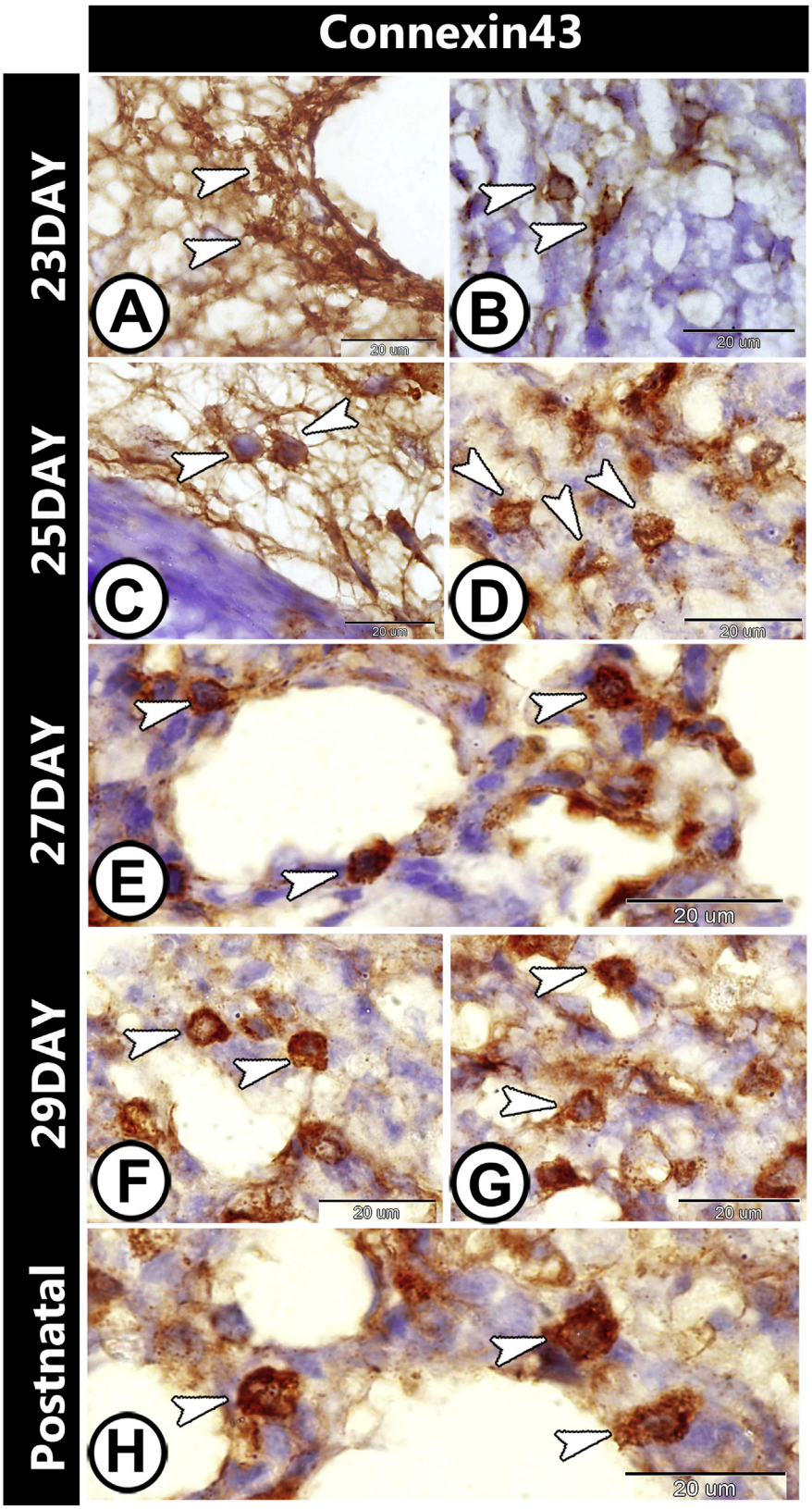

Fig. 5. Immunohistochemical expression pattern of connexin 43 in lung at different developmental ages. A-H: DCs (arrowheads) expressed a strong immunoreactivity to connexin 43 in the wall of developing blood vessels (BV), in pulmonary interstitium (IS), within the wall of developing bronchioles (Br), and within the wall of developing air saccules (AS) or developing alveoli (AL).

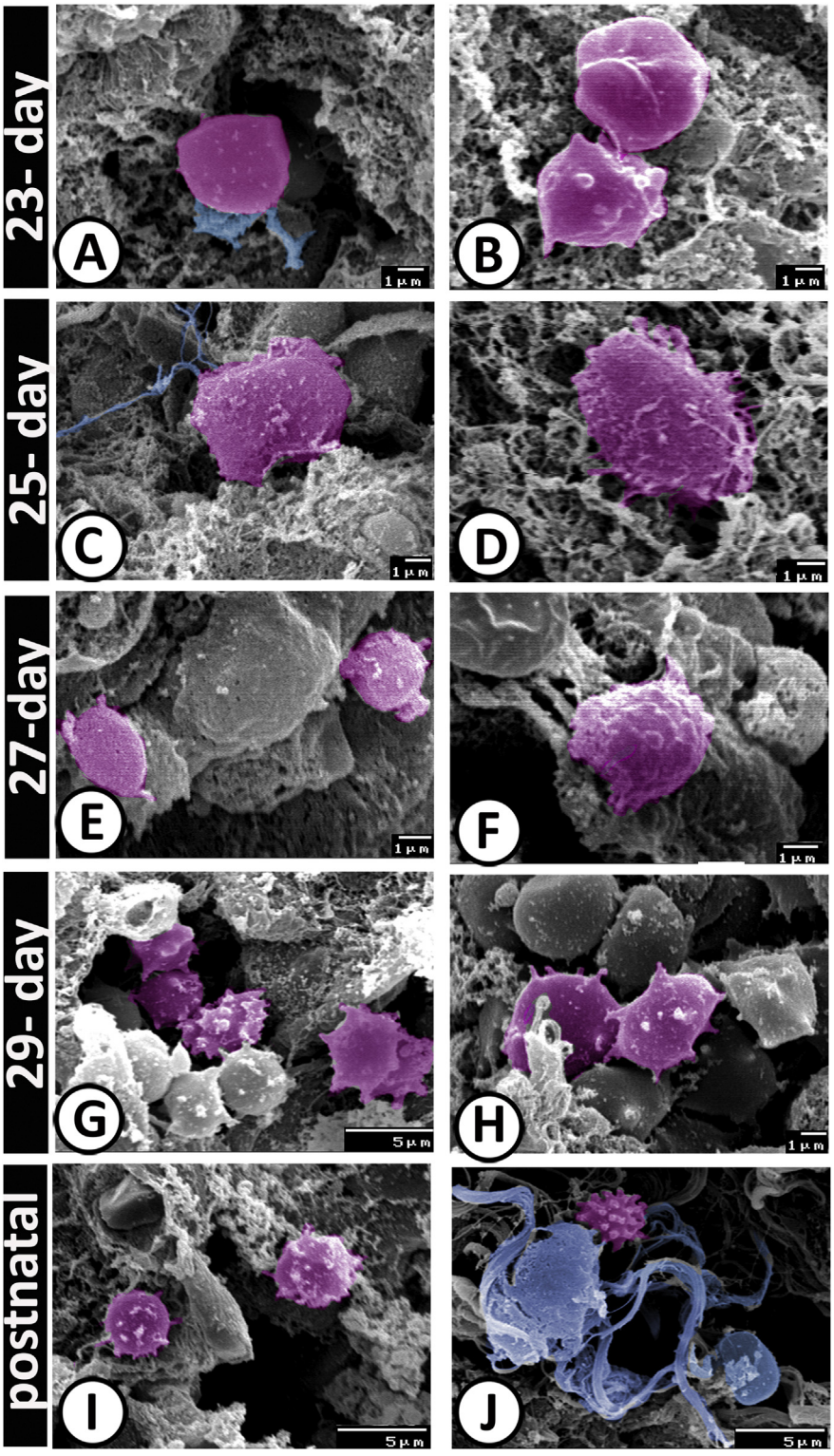

Fig. 6. Digital colored scanning electron microscopy of the developing of the pulmonary DCs (pink):
A, B: On the 23rd gestational day, the DCs were demonstrated around the developing air spaces in association with Tps of TCs (blue). **C, D:** On the 25th gestational day, the DCs enlarged and covered by short microvilli. **E, F:** On the 27th gestational day, the DCs consisted of rounded to oval cell bodies with many short cell processes. **G, H:** On the 29th gestational day, many DCs could be observed in groups and established close contact with each other. **I, J:** In the postnatal period, close contact between the DCs and TCs and their Tps (blue) were demonstrated.

software. The number of $CD8^+$ DCs, $CD56^+$ DCs and $CD34^+$ DCs (per 20 μm^2 using a 100 X objective) were recorded. All the data were presented as the mean ± SE and statistically analyzed using one-way analysis of variance (ANOVA) followed by Duncan's multiple range test to compare the number of DCs/unit area in the five age groups. These data were expressed by Graph Pad Prism (version 6.05; International Scientific Community). Differences were considered significant at $p < 0.05$ and highly significant at $p < 0.01$.

2.6. Detection of the relative percentage of $CD8^+$ DCs co-expressed CD56

Two-step serial sections were selected at 25th gestational day. These

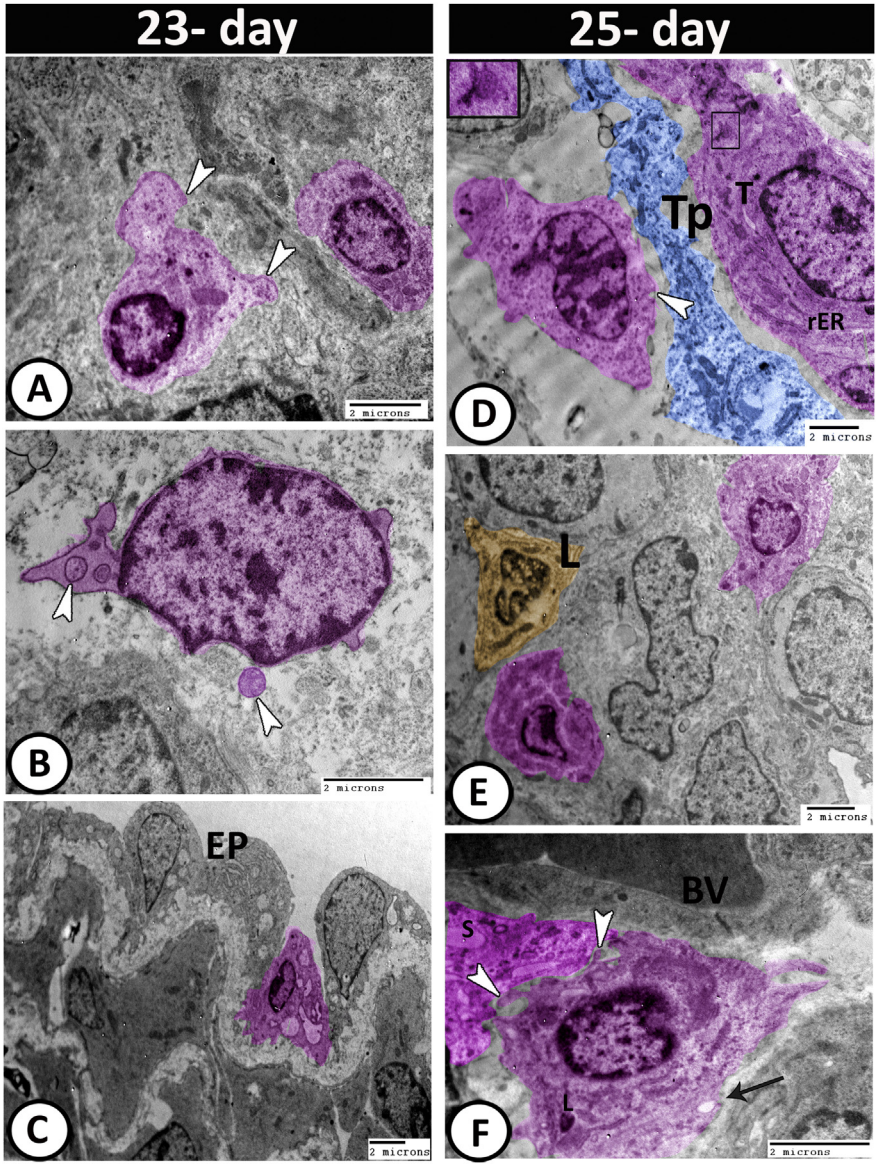

Fig. 7. Digital colored transmission electron microscopy of the pulmonary DCs (pink) on the 23 (A–C) and 25th (D–F) gestational days:
A: The myeloid DCs were characterized by their heterochromatic indented nuclei, abundant cytoplasm and irregular shaped cell bodies with few thick pseudopodia (arrowheads). **B:** Plasmacytoid DCs characterized by the enlarged nucleus and reduced cytoplasm as well as they displayed bulbous-like processes and vesicles (arrowheads) that some of them were released to the interstitium. **C:** Myeloid DC was intermingled between the developing epithelial cells (EP) of the bronchioles. **D:** Myeloid DCs showed signs of endocytosis in the form of distributed tubules (T), caveolae (arrowhead), rER, multivesicular bodies (inserted box) and release of secretory materials to the connective tissues. Note the DCs were recorded in the connective tissues in relation to telopodes of telocytes (blue). **E:** Myeloid DCs were observed in vicinity to lymphocyte (orange). F: plasmacytoid DCs were observed around the blood vessels (BV) of the airways. Note the presence of fine dendrites (arrowheads), vesicles (arrow), lysosome (L) and released secretory products (S).

sections were immunostained by CD8 and CD56, respectively. Five fixed microscopic fields were randomly selected from CD8 immuno-stained sections and $CD8^+$ DCs were quantified in each field and were recorded. Exactly, the same fields were examined in CD56 immunostained section and only $CD8^+$ DCs that co-expressed CD56 were quantified in each field and were recorded too. Then the relative percentage of $CD8^+$ DCs co-expressed CD56 was calculated. The same method was performed in the 7th postnatal day. The same quantification method was also repeated twice again on the same ages using other step-serial sections. Data from both age groups were analyzed using Student's T-Test. These data were expressed by Graph Pad Prism (version 6.05; International Scientific Community).

2.7. Detection of the relative percentage of $CD8^+$ DCs co-expressed NSE, VEGF and Connexin 43

The same above mentioned quantification method was carried out on the same ages using immune-stained step-serial sections.

3. Results

3.1. Light microscopy

At 23rd gestational day, the fetal rabbit lung is in the pseudoglandular stage. At this stage, all the conductive airways are easily distinguished. Each prospective terminal bronchiole branches to give 2–4 straight ducts and each duct ends by a terminal bud. These terminal buds are lined by low columnar cells (Elhafez et al., 2012). At this age, DCs were difficult to be observed in semithin sections.

At 25th gestational day, the fetal lung is in the canalicular stage that marked by a progressive vascularization of the pulmonary interstitial tissue. The first air-blood barrier is formed through close contact of the developing type I pneumocyte with some capillaries (Schittny and Burri, 2007). DCs were recognized sporadically in the interstitial tissue of developing rabbit lung. They appeared as stellate cells with a deeply stained nucleus and deeply stained cytoplasm. They were provided by 1–2 small fine cytoplasmic processes (Fig. 1A).

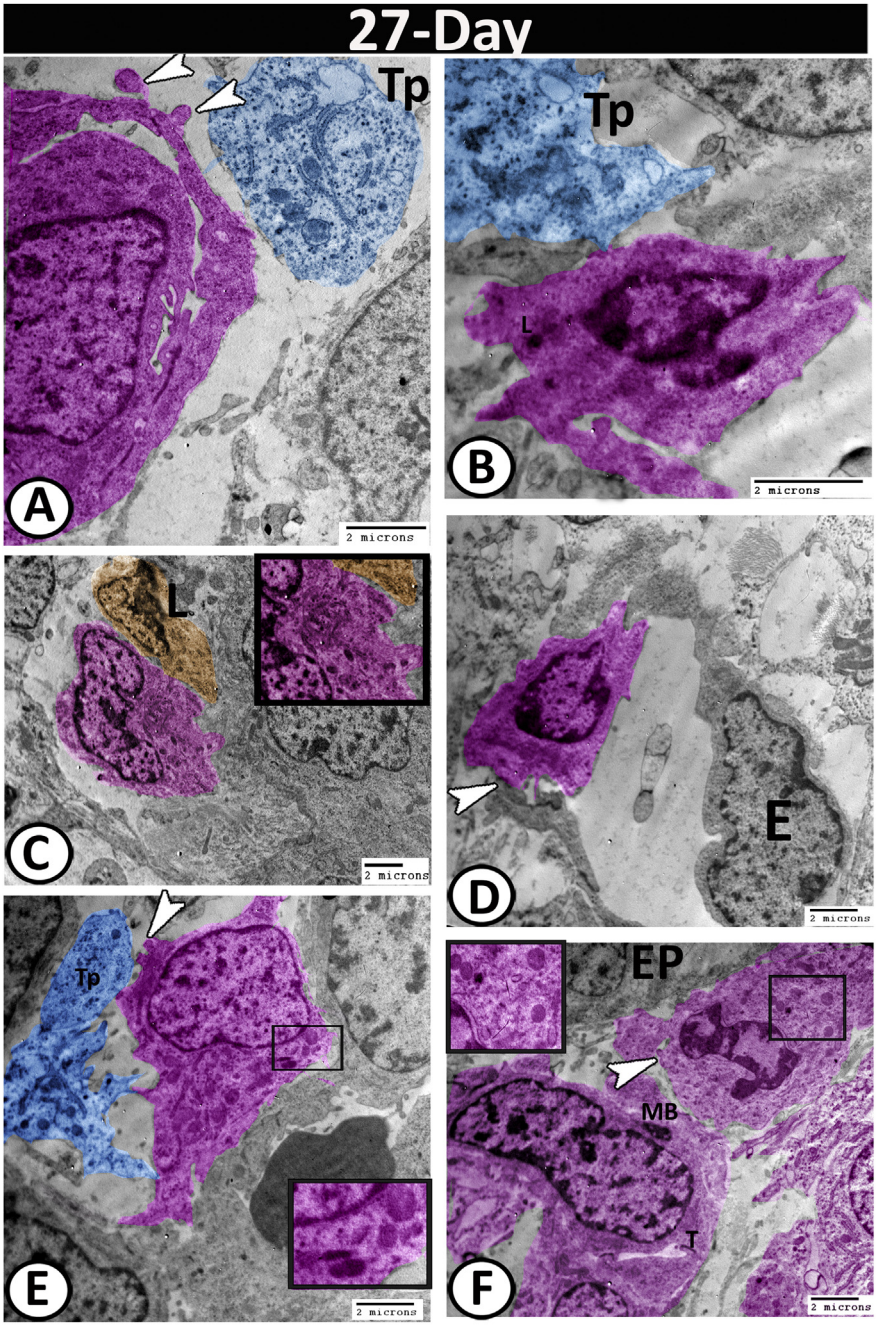

Fig. 8. Digital colored transmission electron microscopy of the pulmonary DCs (pink) on the 27th gestational days:
A, B: DCs showed lysosomes (L) and numerous and long cell processes (arrowheads) that established close contact with Tps of the TCs (blue). **C:** DCs characterized by an indented nucleus, and electron-lucent cytoplasm filled with dense granules, tubules, and rER (inserted box). Note the close contact between DC and lymphocyte (orange). **D:** the plasmacytoid DCs connected by gap junction (arrowhead) with the endothelium (E). **E:** Myeloid DC contained mitochondria, rER, scattered ribosomes and dense granules (inserted box). Note the bridge of dendrites between the Tps (blue) and DCs (arrowhead). **F:** a well-developed myeloid DC was connected directly by their processes with the epithelium (EP) of the bronchioles and contained multivesicular bodies (inserted box, MB), tubules (T) and small secretory vesicles (arrowhead) that some of them were released to the connective tissues.

At 27th gestational day, the fetal lung is in the saccular stage that characterized by the branching of the terminal bronchioles into several ducts that end by air saccules. The thick inter-saccular septa with a characteristic double capillary layer are observed (Schittny and Burri, 2007). DCs were observed in the lamina propria of the bronchioles in a close association to the bronchiolar epithelium (Fig. 1B). They were also recognized within the inter-saccular septa around the air saccules and in the tunica adventitia of growing blood vessels (Fig. 1 C).

At 29th gestational day, the fetal lung is in the alveolar stage. At this age, the air conducting system becomes morphologically and functionally mature. The air saccules are subdivided by developing septa into primitive alveoli (Elhafez et al., 2012). DCs were demonstrated in lamina propria of bronchiolar mucosa in close contact to the bronchiolar epithelium (Fig. 1 D). They were also recognized in the wall of developing blood vessels beneath the endothelial cells (Fig. 1 E).

At 7th postnatal day, the fetal rabbit lung is in the alveolar stage. The pulmonary alveoli appear thin-walled and greatly dilated giving its mature cup-shaped appearance (Mokhtar et al., 2019). DCs were demonstrated extensively in the lamina propria of bronchiolar mucosa (Fig. 1F), in the wall of blood vessels (Fig. 1G), within the interstitial tissue of inter-alveolar septa (Fig. 1H), and surrounding the nerve fibers (Fig. 1 I).

3.2. *Immunohistochemistry*

Immunohistochemical characterization of rabbit pulmonary tissue

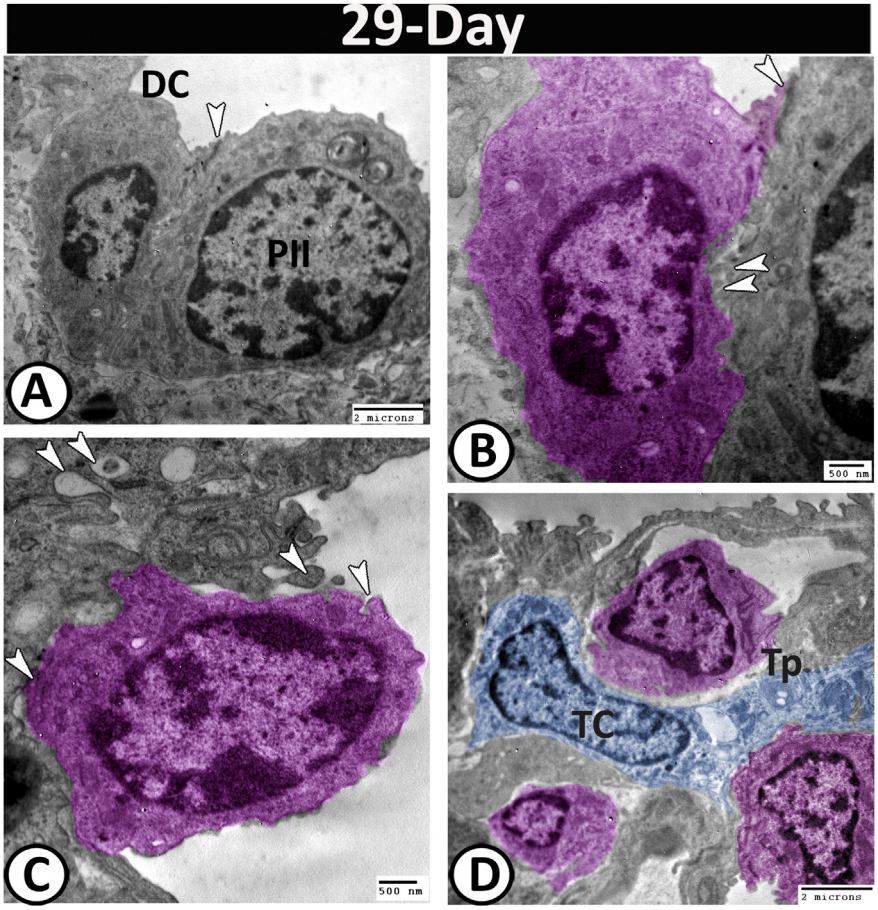

Fig. 9. Digital colored transmission electron microscopy of the pulmonary DCs (pink) on the 29th gestational days:
A, B: Myeloid DCs connected with type II pneumocytes (PII) by tight junction (single arrowhead), dendrites and secretory vesicles (double arrowheads) that extended towards the pneumocytes. **C:** A typical plasmacytoid DC with many cell processes showed endocytic activities with many pearls like caveolae, and coated vesicles and pits (arrowheads). **D:** the DCs established close contact with Tps and TCs cell bodies (blue).

during different developmental stages revealed a clear wide variation in density, distribution, and activity of DCs. DCs showed strong immunoreactivity for both CD8 (Fig. 2) and CD56 (Fig. 3A–E) at all developmental ages. The frequency of immunoreactive cells and their staining density increased gradually with the advancement of age. $CD8^+$ DCs and $CD56^+$ DCs were demonstrated in bronchiolar mucosa, within the adventitia of developing blood vessels and within pulmonary interstitium (Figs. 2 and 3A-E). Their fine dendrites extended to make a connection with each other and with telocytes forming characteristic networks. Moreover, some DCs strongly expressed CD34 within the lining epithelium of developing airways protruding to the lumen, within the wall of developing blood vessels, and in the pulmonary interstitial tissue (Fig. 3F–J). Their dendrites showed a fine connection to other DCs and TCs. However, it was clear that the frequency of $CD34^+$ DCs was much lesser than that of $CD8^+$ DCs and $CD56^+$ DCs at all developmental ages. VEGF was expressed in DCs in the interstitial tissue of inter-saccular or inter-alveolar septa during all developmental stages and they showed a close vicinity to the developing blood vessels and the developing alveoli (Fig. 4A–E). In addition, DCs expressed NSE in the pulmonary interstitial tissue of inter-saccular or inter-alveolar septa and within the developing alveoli protruding to the alveolar lumen (Fig. 4F–J). DCs in rabbit lungs expressed also a strong reactivity to connexin 43 at the level of both the cell bodies and their dendrites at all developmental ages (Fig. 5).

3.3. Scanning electron microscopy

On the 23rd gestational day, the dendritic reticular cells (DCs) were demonstrated around the developing air spaces in association with telopodes (Tps) of telocytes (TCs). They were polyhedral in shape with short cell processes (Fig. 6A and B). On the 25th gestational day, the dendritic cells enlarged and covered by short microvilli (Fig. 6C and D). On the 27th gestational day, the dendritic cells exhibited a mature appearance in the form of rounded to oval cell bodies with many short cell processes (Fig. 6E and F). On the 29th gestational day, many DCs could be observed in groups and established close contact with each other (Fig. 6G and H). In the postnatal period, the DCs were numerous. Close contact between the DCs and TCs and their Tps were demonstrated (Fig. 6I and J).

3.4. Transmission electron microscopy

Rogers et al. (2008) identified the myeloid DCs by the presence of pseudopodia, nuclear indentation with the peripheral arrangement of heterochromatin and abundance of cytoplasm. On the other hand, plasmacytoid DCs characterized by many projections, reduced cytoplasm and heterochromatic nucleus (Schuller et al., 2013).

On the 23rd gestational day, the dendritic reticular cells (DCs) were recognized in the interstitium among the connective tissue cells (Fig. 7A and B) or intermingled between the developing epithelial cells of the bronchioles and bulging to the lumen (Fig. 7C). The myeloid DCs were characterized by their heterochromatic indented nuclei, abundant cytoplasm and irregular shaped cell bodies with few thick cell processes or pseudopodia (Fig. 7A). Plasmacytoid DCs characterized by the enlarged nucleus and reduced cytoplasm as well as they displayed a bulbous-like processes (Fig. 7B). The cytoplasm of both types contained few mitochondria, rER, electron-dense secretory granules and membrane-

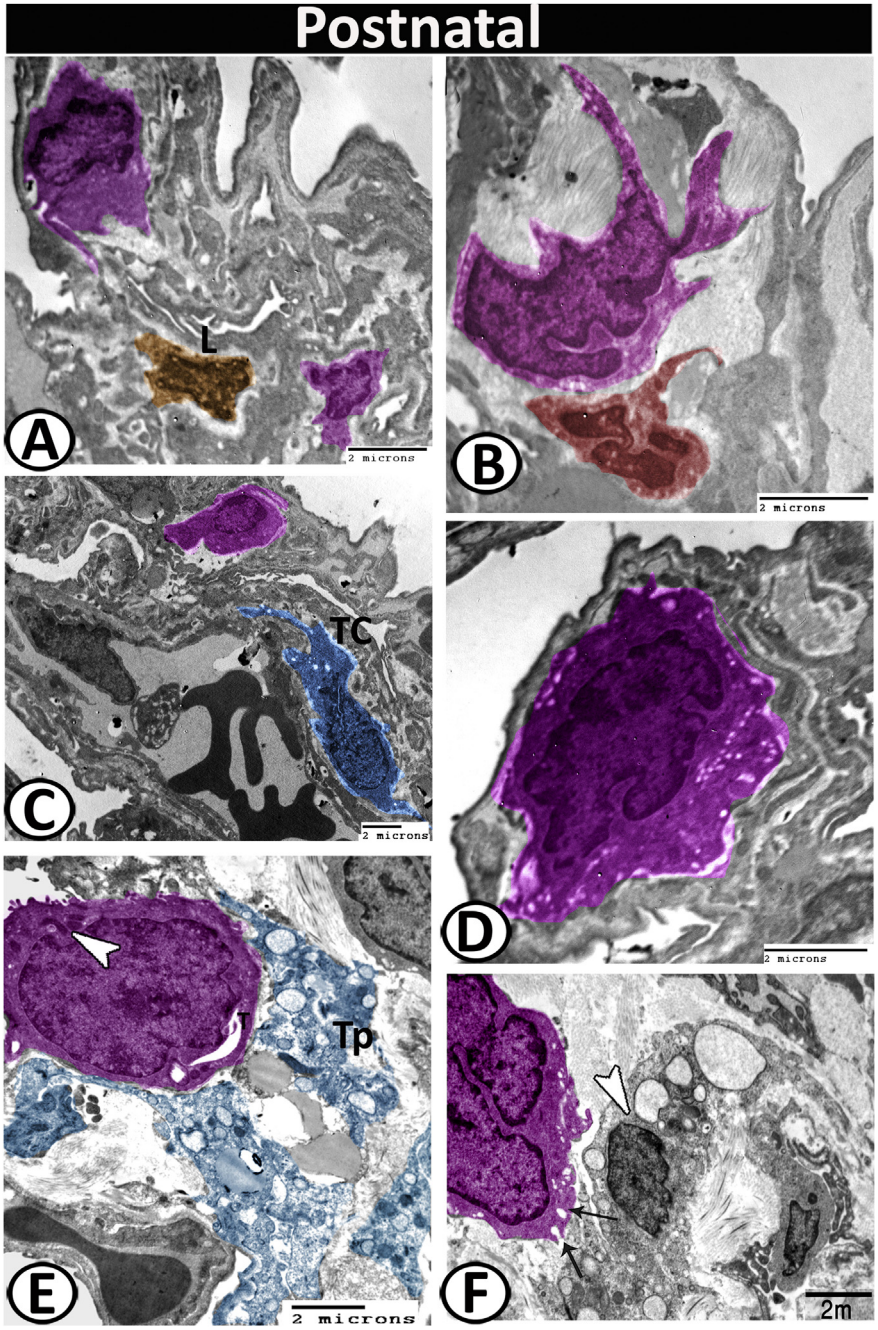

Fig. 10. Digital colored transmission electron microscopy of the pulmonary DCs (pink) in the postnatal life:
A-C: DCs were observed in the interstitium in association with lymphocytes (orange), and neutrophils (red) and around the blood vessels in vicinity to telocytes (blue). **D:** plasmacytoid DCs contained many endocytic vesicles. **E:** The DCs cells characterized by numerous fine dendrites, high nuclear to cytoplasmic ratio and their cytoplasm contained tubules (T) and Birbeck granules (arrowhead). Note the Tps of TCs were partially encircled the DC (blue). **F:** DCs observed in relation to apoptotic cells (arrowhead) and showed high endocytotic activities and release their secretory vesicles toward these cells (arrows).

bounded vesicles (Fig. 7A–C). Some of these cells shown to release coated secretory vesicles to the connective tissues (Fig. 7B).

The 25th gestational day acted as a point of change for the DCs. They showed the beginning of the formation of dendrite-like processes and their cytoplasm contained profiles of rER, scattered ribosomes and dense granules (Fig. 7D, F). Moreover, in this age, we found signs of endocytosis in form of distributed vesicles, tubules, caveolae, lysosomes and multivesicular bodies and release of secretory materials to the connective tissues (Fig. 7D, F). Myeloid DCs were recorded in the connective tissues in relation to telopodes of telocytes (TCs) (Fig. 7D), lymphocyte (Fig. 7E), and around the blood vessels of the respiratory portion of the lung (Fig. 7F).

On the 27th gestational day, the nuclear membrane showed many indentations. The cytoplasm was abundant, electron-lucent and filled with dense granules, multivesicular bodies, tubules, lysosomes, mitochondria, rER and small secretory vesicles that some of them were released to the connective tissues. Their cell processes increased in number and length that formed close contact with Tps of the TCs (Fig. 8A, B, E) and with lymphocytes (Fig. 8C). Moreover, the plasmacytoid DCs may contribute to the angiogenesis as they connected by gap junction with the endothelium to form the new blood vessels (Fig. 8D). In addition, a well-developed myeloid DC was connected directly by their processes with the epithelium of the bronchioles (Fig. 8F).

On the 29th gestational day, the DCs showed an obvious increase in the nuclear/cytoplasmic ratio. The myeloid DCs exhibited a unique connection with type II pneumocytes and bulging to the lumen of the alveoli. They connected with it by a tight junction, in addition to dendrites and secretory vesicles that extended towards the pneumocytes. The

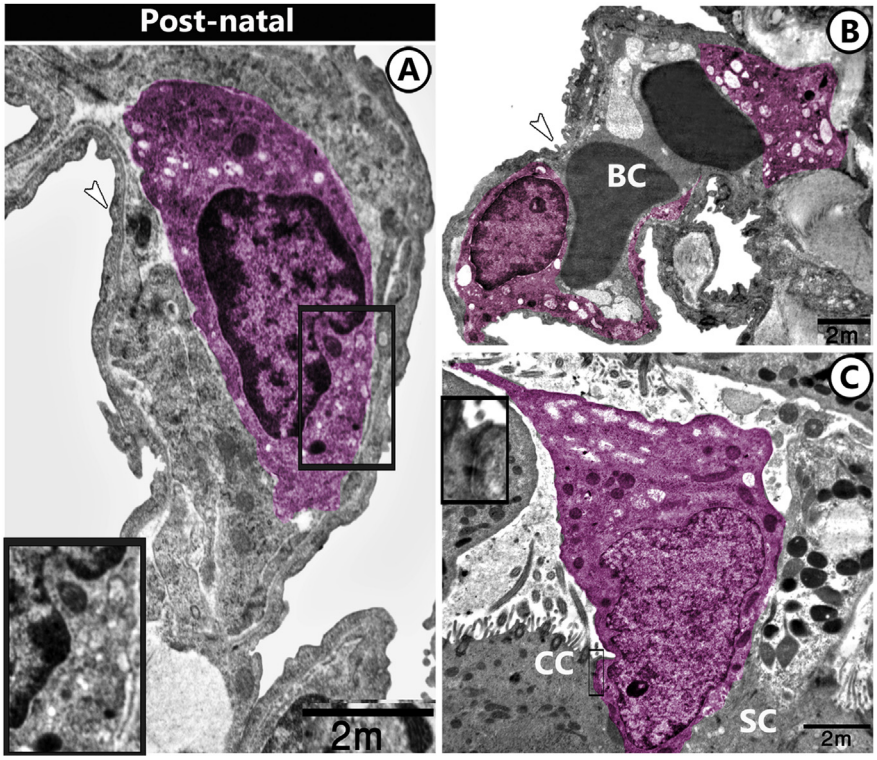

Fig. 11. Digital colored transmission electron microscopy of the pulmonary DCs (pink) in the postnatal life:
A: DC is in a close association with the air-blood barrier of the lung (arrowhead). They characterized by their extensive endosomal systems that included multivesicular bodies, lysosomes, many vesicles and caveolae (inserted box). **B:** DC is in a close association with the air-blood barrier of the lung (arrowhead). Note release of some secretory vesicles and dense granules to the pulmonary blood capillaries (BC). **C:** DC is among the ciliated (CC) and secretory cells (SC) of the bronchiole. The DC was connected with the bronchiolar epithelium by both tight junction and desmosomes (inserted box).

cytoplasm contained many mitochondria, rER and numerous glycogen dense granules (Fig. 9A and B). A typical plasmacytoid DC with many cell processes was bulged to the lumen of the air spaces and showed endocytic activities with many pearls like caveolae, and coated vesicles and pits (Fig. 9C). Moreover, the DCs established close contact with Tps and TCs cell bodies (Fig. 9D).

In the postnatal period, both myeloid (Fig. 10 A, C) and plasmacytoid DCs (Fig. 10B, D, E, F) were observed. The DCs cells reached the mature appearance and showed an obvious increase in their number and they characterized by numerous fine dendrites, and high nuclear to cytoplasmic ratio (Fig. 10A–D). Some of these cells showed spiny or claw-like cell processes (Fig. 10B). While the others, their cytoplasm possessed the characteristic club-shaped electron-dense secretory granules (Birbeck granules) and many endocytic vesicles (Fig. 10D and E). The nucleus was indented and possessed peripheral heterochromatin. They were observed in association with wondering white blood cells (neutrophils) (Fig. 10B) and telocytes (Fig. 10C). DCs appeared to have a role in apoptosis as they observed in relation to apoptotic cells and showed high endocytotic activities and release their secretory vesicles toward these cells (Fig. 10F).

Moreover, DCs were demonstrated in a close association with the air-blood barrier of the lung (Fig. 11A and B). They characterized by their extensive endosomal systems and release of some secretory vesicles and dense granules to the pulmonary blood capillaries (Fig. 11B). In addition, a unique appearance of the dendritic cell among the ciliated and secretory cells of the bronchioles was recorded as it bulged toward the lumen. They were distinguished by the presence of numerous vesicles, mitochondria, and many scattered dense bodies. The DC was connected with the bronchiolar epithelium by both tight junction and desmosomes (Fig. 11C).

3.5. Morphometrical and statistical analysis

The present morphometrical and statistical data showed a significant increase in the number of $CD8^+$ DCs, $CD56^+$ DCs and $CD34^+$ DCs at 7th postnatal day compared to 23rd and 25th gestational day (Fig. 12). The frequency of $CD34^+$ DCs was much lesser than that of $CD8^+$ DCs and $CD56^+$ DCs at all developmental ages (Fig. 12). On the other hand, $CD8^+$ DCs showed a clear positive co-expression of CD56 and the other non-specific markers (VEGF, NSE and Connexin 43) in both prenatal and postnatal groups (Fig. 13). No significant variance was recorded in the relative co-expression % of $CD8^+$ DCs to those markers between the two age groups. (Fig. 13).

4. Discussion

Dendritic cells in the lung are believed to be the most potent APCs functionally specialized in the uptake, transport, and presentation of Ags and have the unique capacity to stimulate naive and memory T cells and thus, control airway inflammation. Moreover, DCs can interact with NK cells and B cells (Holt et al., 1988; van Rijt et al., 2002; Huh et al., 2003). Recently, respiratory tract-DCs receive considerable attention as a potential target for many immunotherapy respiratory disease. No available literature were found on the ultrastructural and immunohistochemical development of dendritic cells.

Dendritic cells (DCs) comprise a complex system of cells with various anatomical localization, distinct subsets, and different functions (Steinman, R. M. 1991). DCs are distributed in both lymphoid and non-lymphoid tissues. All types of DCs developed in the bone marrow and migrated to the tissues, including the lung, in an immature form (Holt and Stumbles, 2000). The migratory DCs possessed a great ability to induce T cell-mediated immune responses due to their capacity to capture antigens and migrate via afferent lymphatics into the draining LN where they interact with naïve T cell leading to antimicrobial, antitumoral, and allergic immune responses [Steinman and Hemmi, 2006].

The distribution of DCs in the lung has been examined in mice, rats and human [Holt et al., 1988; Van Haarst et al., 1994; Lambrecht et al., 1998]. The current study revealed that the DCs in the bronchioles formed a tight network with the epithelium, lamina propria, adventitia, whereas in the lung parenchyma they were found in alveolar spaces, bulging to the alveolar lumen and in the connective tissues surrounding the blood vessels and pleura. These locations allow DCs to initiate the immune responses to inhaled antigens, viruses and bacteria. The present study

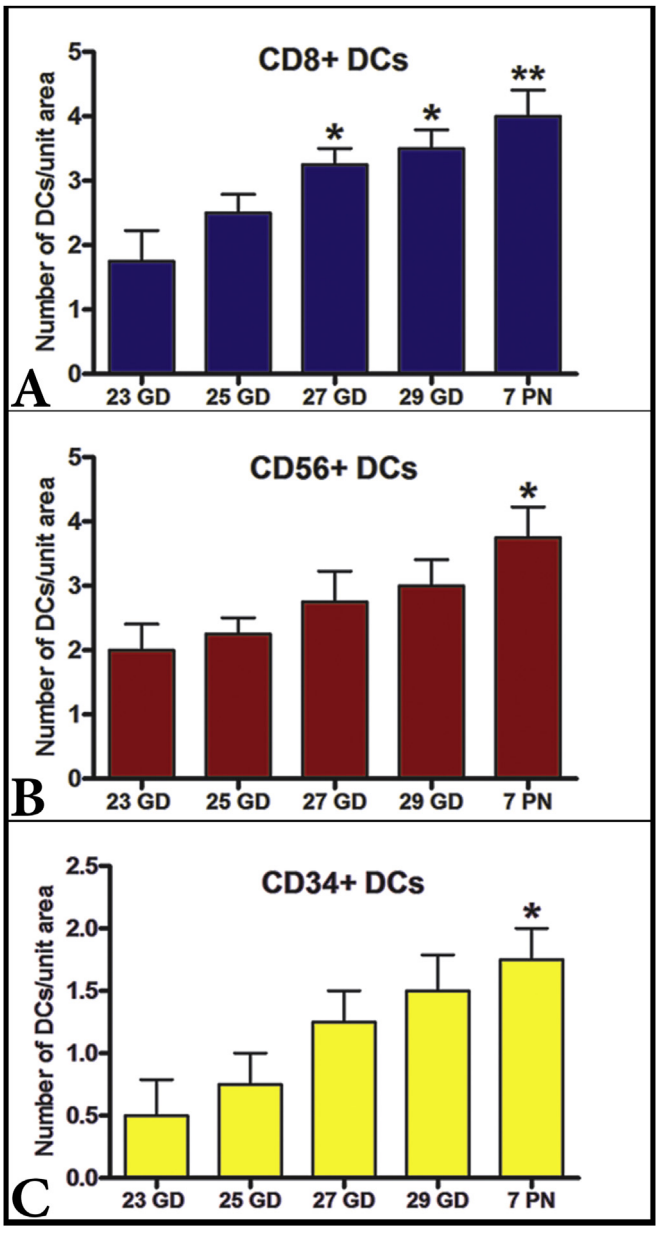

Fig. 12. The statistical analysis of DCs number/unit area at different developmental ages
. **A:** Number of $CD8^+$ DCs **B:** Number of $CD56^+$ DCs **C:** Number of $CD34^+$ DCs.

demonstrated the association of dendritic cells with a network of nerve endings. This network comprises active neuromediators such as calcitonin-gene-related peptide (CGRP) and substance P that are essential for the crosstalk between nervous and immune systems (Lambrecht et al., 1999).

Lung DCs are the major producers of chemokines involved in the recruitment of T cells, and neutrophils not only in a steady state but also upon stimulation with airway-borne antigens (Beaty et al., 2007). The present study revealed that postnatal DCs showed the capacity to carry out endocytosis toward an apoptotic cell. The clearance of apoptotic cells is a major mechanism that allows DCs to present self-antigens for the maintenance of self-tolerance (Miyake et al., 2007). The endosomal pathway in the dendritic cells consisted of vesicular and tubular lipid bodies (Compeer and Boes, 2014). Moreover, the current result revealed that the developing DCs showed active endocytosis in form of formation of many coated vesicles, caveolae and release of the secretory materials to the pulmonary interstitium and thus may be efficient in antigen uptake but may have the low ability in T-cell stimulation.

The current study revealed that on the 23, and 25th gestational days, the DCs characterized by single profiles of rER and scattered ribosomes, suggesting a low protein synthesis capability and the consequent limited ability of these cells to promote strong T-cell presentation. On the other hand, the presence of these cells in the fetal lung may indicate that these DCs may have a role in the proliferation and this suggestion may be support by their strong positive expressions of CD34 in the fetal and early neonatal life which indicated that DCs may be involved in the mesenchymal cells differentiation and in pulmonary angiogenesis. CD34 is a typical marker for blood progenitor cells (Eidenschink et al., 2012), and many undifferentiated cells (Sidney et al., 2014).

Post-natal DCs and 29th gestational days showed signs of intensive protein synthesis in the form of enlarged mitochondria, many cisternae of rER and numerous vacuoles. Moreover, the mature DCs contained vesicles and multivesicular bodies that act the main sites of endocytosis for antigens (West et al., 1994). The vesicles had an important role in the transportation of peptide complexes to the plasma membrane and as a storage site to many secreting immunoregulatory factors from DCs. Also, these vesicles play a significant role after antigen processing as they act as accumulation sites for T-cells receptors legends (Turley et al., 2000).

Moreover, the difference in the morphological characters of all studied dendritic cells may be related to their developmental stage or the activation state and so reflected different functional roles (El Shikh et al., 2006). The plasmacytoid DCs are highly secreting cells to interferon-α during the viral infection and they prevent replications of cancer cells and kill them in a contact-dependent fashion (Rogers et al., 2008).

Recently, $CD8^+$ DCs are considered as independent DC subpopulations both functionally and ontogenetically. $CD8^+$ DCs represent the last stage of DC differentiation, playing a major role in the stimulation of T-cell responses, due to their antigen-presenting potential, cross-priming capacity, and ability to secrete various cytokines such as interferon γ and interleukin-12 (Hoyo et al., 2002). $CD8\alpha^+$ DC is considered a plasmacytoid-derived (lymphoid derived) population (Banchereau et al., 2000). The current study showed that $CD8^+$ DCs present pDCs morphology in the form of many cell projections and reduced cytoplasm and many of these immunoreactive cells were demonstrated in the postnatal life. Iyoda et al. (2002) added that splenic $CD8^+$ DCs are the major DC populations involved in the uptake of apoptotic bodies from peripheral blood.

CD56 is the phenotypic marker of natural killer cells but it can be expressed by many other immune cells, such as T cells, dendritic cells, and monocytes (Van Akar et al 2017). Unfortunately, very little is known regarding the functional role of CD56 on immune cells. CD56 plays a critical role in the development of NK cells and in the establishment of its developmental synapses (Mace et al., 2016). It was found that blocking of CD56 could affect both NK cell motility and maturation (Mace et al., 2016). Moreover, it was recorded that $CD56^+$ immune cells are also able to form strong immune synapses with each other through CD56 binding, for example, $CD56^+$ DCs have been shown to induce the preferential activation and expansion of $CD56^+$ γδ T cells via CD56 (Nieda et al., 2015). Our morphometrical data showed a significant increase in the number of $CD56^+$ DCs/unit area with the advancement of age. We suggest that CD56 strongly affect the maturation and migratory behavior of DCs in the developing rabbit lung.

The present study revealed that DCs express connexin-43 for the first time and this expression increased by the advancement of the age and this observation was supported by the ultrastructural findings as we found a well-distinct gap junction between the DC and vascular endothelium that may facilitate the transport of small molecules from DCs. In addition, a tight junction was demonstrated between the dendritic cells and pneumocytes. Also, tight junction and desmosomes were recognized between the DCs and bronchiolar epithelium. These junctions may help in holding of the dendritic cells in place or in the formation of a network to maximize their action. DCs were NSE-positive and this may due to that

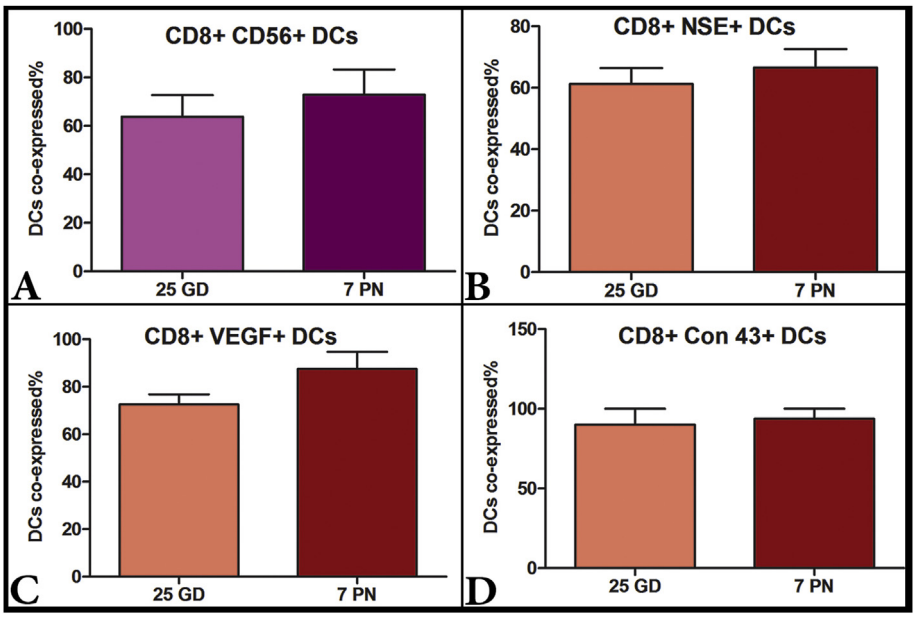

Fig. 13. The statistical analysis of relative percentage CD8$^+$ DCs co-expression at 25th gestational day and 7th postnatal day
. **A:** Relative percentage of CD8$^+$ CD56$^+$ DCs **B:** Relative percentage of CD8$^+$ NSE$^+$ DCs **C:** Relative percentage of CD8$^+$ VEGF$^+$ DCs. **E:** Relative percentage of CD8$^+$ Con 43$^+$ DCs.

enolase were present on the cell surface of the activated immune cells, where it acts as plasminogen receptor and promoting autoimmunity (Bae et al., 2012).

The telocytes (TCs) are unique interstitial cells that are discovered recently and implicated in many functional roles. The current study revealed that the DCs were in close contact with TCs in all developmental stages of the lung. In addition, the present study supported our previous investigation (Hussein and Mokhtar, 2018) that the DCs and TCs appear to involve in the angiogenesis as we observed a gap junction between the DC and vascular endothelium. This observation is also confirmed by positive-immunoreactions for VEGF in the DCs. The expression of VEGF in the DCs is critical as this growth factor is considered as an angiogenic factor that stimulates the vascular permeability and the proliferation of the vascular endothelium (Keck et al., 1989).

In conclusion, the application of transmission electron microscopy in the current study allows identification of all populations of the DCs. The difference in the maturation status may reflect different roles for DCs in the lung. Our findings suggest that immature DCs may have an antigen-uptake role through endocytosis, while mature DCs may involve in antigen presentation to T-cells.

Ethical approval and consent to participate

The study was approved by the Ethics Committee of Assiut University, Egypt.

Consent for publication

Not applicable.

Availability of data and materials

The datasets used and/or analyzed during the current study are available from the corresponding author on reasonable request.

Competing interests

The authors declare that they have no competing interests.

Funding

The current study hasn't any fund from any organizations or institutions.

Acknowledgments

The authors thank Dr. Ramy Kamal, a lecturer of anatomy at Sohag University, for his co-operation in the morphometric study. This work was supported by Faculty of Veterinary Medicine, Assiut University, Egypt.

List of abbreviations

NK	Natural killer
NSE	Neuron-specific enolase
rER	rough endoplasmic reticulum
SEM	Scanning electron microscopy
TCs	telocytes
TEM	transmission electron microscopy
Tps	telopodes
VEGF	Vascular endothelial growth factor
Con 43	Connexin 43

References

Bae, S., Kim, H., Lee, N., Won, C., Kim, H.R., Hwang, Y.I., Song, Y.W., Kang, J.S., Lee, W.J., 2012. Alpha-Enolase expressed on the surfaces of monocytes and macrophages induces robust synovial inflammation in rheumatoid arthritis. J. Immunol. 189, 365–372.

Banchereau, J., Briere, F., Caux, C., Davoust, J., Lebecque, S., Liu, Y.J., Pulendran, B., Palucka, K., 2000. Immunobiology of dendritic cells. Annu. Rev. Immunol. 18, 767–811.

Beaty, S.R., Rose Jr., C.E., Sung, S.S., 2007. Diverse and potent chemokine production by lung CD11bhigh dendritic cells in homeostasis and in allergic lung inflammation. J. Immunol. 178, 10882–10895.

Buczkowski, J., Rolinski, J., Krawczyk, P., Tabarkiewicz, J., Kieszko, R., Michnar, M., Milanowski, J., 2002. The role of myeloid and lymphoid blood dendritic cells in modulating Th1/Th2 balance in sarcoidosis. Ann. Univ. Mariae Curie Sklodowska (Medicina) 58, 137–141.

Compeer, E.B., Boes, M., 2014. MICAL-L1-related and unrelated mechanisms underlying elongated tubular endosomal network (ETEN) in human dendritic cells. Commun. Integr. Biol. 7, 6.

Demangel, C., Bean, A.G.D., Martin, E., Feng, C.G., Kamath, A.T., Britton, W.J., 1999. Protection against aerosol Mycobacterium tuberculosis infection using Mycobacterium bovis Bacillus Calmette Guerin-infected dendritic cells. Eur. J. Immunol. 29, 1972–1979.
Dudziak, D., et al., 2007. Differential antigen processing by dendritic cell subsets in vivo. Science 315, 107–111.
D'Hulst, A., Vermaelen, K.Y., Pauwels, R.A., 2002. Cigarette smoke exposure causes increase in pulmonary dendritic cells. Am. J. Respir. Crit. Care Med. 165, A604.
Eidenschink, L., DiZerega, G., Rodgers, K., et al., 2012. Basal levels of CD34 positive cells in peripheral blood differ between individuals and are stable for 18 months. Cytom. B Clin. Cytom. 82, 18–25.
Elhafez, E.A.A., Mohamed, G.A., Hussein, M.M., 2012. Development of the respiratory acinus in the rabbit lung. Recent Res. Med. Med. Chem. 01, 14–17.
ElShikh, M.E., El Sayed, R., Szakal, A.K., Tew, J.G., 2006. FDC-FcgRIIB engagement via immune complexes induces the activated FDC phenotype associated with secondary follicle development. Eur. J. Immunol. 36, 2715–2724.
Hansen, M., Andersen, M.H., 2017. The role of dendritic cells in cancer. Semi. Immunopathol. 39, 307–316.
Holt, P.G., Stumbles, P.A., 2000. Regulation of immunologic homeostasis in peripheral tissues by dendritic cells: the respiratory tract as a paradigm. J. Allergy Clin. Immunol. 105, 421–429.
Holt, P.G., Schon-Hegrad, M.A., Oliver, J., 1988. MHC class II antigen-bearing dendritic cells in pulmonary tissues of the rat. Regulation of antigen presentation activity by endogenous macrophage populations. J. Exp. Med. 167, 262–274.
Hoyo, G.M., Martín, Pilar, Fernańdez Arias, Cristina, Alvaro Rodríguez Marín, Ardavín, Carlos, 2002. CD8α$^+$ dendritic cells originate from the CD8α$^+$ dendritic cell subset by a maturation process involving CD8α, DEC-205, and CD24 up-regulation. Blood 99, 999–1004.
Hsu, S.M., Raine, L., Fanger, H., 1981. Use of avidin- biotin- peroxidase complex (ABC) in immznoperoxidase techniques. J. Histochem. Cytochem. 29, 577–580.
Huh, J.C., Strickland, D.H., Jahnsen, F.L., Turner, D.J., Thomas, J.A., Napoli, S., Tobagus, I., Stumbles, P.A., Sly, P.D., Holt, P.G., 2003. Bidirectional interactions between antigen-bearing respiratory tract dendritic cells (DCs) and T cells precede the late phase reaction in experimental asthma: DC activation occurs in the airway mucosa but not in the lung parenchyma. J. Exp. Med. 198, 19–30.
Hussein, M.M., Mokhtar, D.M., 2018. The roles of telocytes in lung development and angiogenesis: an immunohistochemical, ultrastructural, scanning electron microscopy and morphometrical study. Dev. Biol. 443, 137–152.
Iyoda, T., et al., 2002. The CD8+ dendritic cell subset selectively endocytoses dying cells in culture and in vivo. J. Exp. Med. 195, 1289–1302.
Karnovsky, M.J., 1965. A formaldehyde-glutaraldehyde fixative of high osmolarity for use in electron microscopy. Cell Biol. 27 (137A).
Keck, P.J., Hauser, S.D., Krivi, G., Sanzo, K., Warren, T., Feder, J., Connolly, D.T., 1989. Vascular permeability factor, an endothelial cell mitogen related to PDGF. Science 246, 1309–1312.
Koshy, S., Indrasingh, I., Vettivel, S., 2003. Dendritic cells in the airways of laboratory Guinea pig and rabbit: a light microscopic zinc lodide-osmium study. J. Anat. Soc. India 52 (1), 42–45.
Lagranderie, M., Nahori, M.A., Balazuc, A.M., Kiefer-Biasizzo, H., Lapa e Silva, J.R., Milon, G., Marchal, G., Vargaftig, B.B., 2003. Dendritic cells recruited to the lung shortly after intranasal delivery of Mycobacterium bovis BCG drive the primary immune response towards a type 1 cytokine production. Immunology 108, 352–364.
Lambrecht, B.N., Hammad, H., 2003. Taking our breath away: dendritic cells in the pathogenesis of asthma. Nat. Rev. Immunol. 3, 994–1003.
Lambrecht, B.N., Salomon, B., Klatzmann, D., Pauwels, R.A., 1998. Dendritic cells are required for the development of chronic eosinophilic airway inflammation in response to inhaled antigen in sensitized mice. J. Immunol. 160, 4090–4097.
Lambrecht, B.N., Germonpre, P.R., Everaert, E.G., et al., 1999. Endogenously produced substance P contributes to lymphocyte proliferation induced by dendritic cells and direct TCR ligation. Eur. J. Immunol. 29, 3815–3825.
Liu, Y.J., 2001. Dendritic cell subsets and lineages, and their functions in innate and adaptive immunity. Cell 106, 259–262.
Liu, Y.J., 2005. IPC: professional type 1 interferon-producing cells and plasmacytoid dendritic cell precursors. Annu. Rev. Immunol. 23, 275–306.
Liu, K., Nussenzweig, Michel C., 2010. Development and homeostasis of dendritic cells. Eur. J. Immunol 40 (8), 2099–2102.
Mace, E.M., Gunesch, J.T., Dixon, A., Orange, J.S., 2016. Human NK cell development requires CD56-mediated motility and formation of the developmental synapse. Nat. Commun. 7, 12171. https://doi.org/10.1038/ncomms12171 93.
McGovern1, N., Jerry, K., Chan, Y., Ginhoux, F., 2014. Dendritic cells in humans—from fetus to adult international immunology, 27 (2), 65–72.
Merad, M., Sathe, P., Helft, J., Miller, J., Mortha, A., 2013. The dendritic cell lineage: ontogeny and function of dendritic cells and their subsets in the steady state and the inflamed setting. Annu. Rev. Immunol. 31, 563–604.
Miyake, Y., Asano, K., Kaise, H., Uemura, M., Nakayama, M., Tanaka, M., 2007. Critical role of macrophages in the marginal zone in the suppression of immune responses to apoptotic cell-associated antigens. J. Clin. Investig. 117, 2268–2278.
Mokhtar, D.M., Hussein, Manal T., Hussein, Marwa M., Enas, A., Abd-Elhafez, Gamal Kamel, 2019. New insight into the development of the respiratory acini in rabbits: morphological, electron microscopic studies, and TUNEL assay. J. Microsc. Microanal. 1–17. https://doi.org/10.1017/S1431927619000059.
Nieda, M., Terunuma, H., Eiraku, Y., Deng, X., Nicol, A.J., 2015. Effective induction of melanoma-antigen-specific CD8+ T cells via Vgamma9gammadeltaT cell expansion by CD56(high+) interferon-alpha-induced dendritic cells. Exp. Dermatol. 24 (1), 35–41. https://doi.org/10.1111/exd.12581.
Reynolds, E.S., 1963. The use of lead citrate at high pH as an electron-opaque stain in electron microscopy. Cell Biol. 17, 208–212.
Rogers, A.V., Ädelroth, E., Hattotuwa, K., Dewar, A., Jeffery, P.K., 2008. Bronchial mucosal dendritic cells in smokers and ex-smokers with COPD: an electron microscopic study. Thorax 63, 108–114.
Schittny, J.C., Burri, P.H., 2007. Development and growth of the lung. Development 139, 111–124.
Schüller, S.S., Sadeghi, K., Wisgrill, Lukas, Dangl, A., Diesner, S.C., Prusa, A.R., Klebermasz-Schrehof, K., Greber-Platzer, S., Neumüller, J., Helmer, H., Husslein, P., Pollak, A., Spittler, A., Förster-Waldl, E., 2013. Preterm neonates display altered plasmacytoid dendritic cell function and morphology. J. Leucoc. Biol. 93.
Shamoto, M., Qian, B., Niimi, H., 1999. Morphological characteristics of dendritic cells. Electron. Microsc. 34, 26–29.
Shortman, K., Liu, Y.J., 2002. Mouse and human dendritic cell subtypes. Nat. Rev. Immunol. 2, 151–161.
Sidney, L.E., Branch, M.J., Dunphy, S.E., et al., 2014. Concise review: evidence for CD34 as a common marker for diverse progenitors. Stem Cell. 32, 1380–1389.
Steinman, R.M., Hemmi, H., 2006. Dendritic cells: translating innate to adaptive immunity. Curr. Top. Microbiol. Immunol. 311, 17–58.
Teunissen, M.B., 1992. Dynamic nature and function of epidermal Langerhans cells in vivo and in vitro: a review, with emphasis on human Langerhans cells. Histochem. J. 24, 697–716.
Thurmon, J.C., Tranquilli, W.J., Benson, G.J., 1996. Lumb & Jones Veterinary Anesthesia, third ed. Lea & Febiger, London.
Todate, A., Chida, K., Suda, T., Imokawa, S., Sato, J., Ide, K., Tsuchiya, T., Inui, N., Nakamura, Y., Asada, K., et al., 2000. Increased numbers of dendritic cells in the bronchiolar tissues of diffuse panbronchiolitis. Am. J. Respir. Crit. Care Med. 162, 148–153.
Turley, S.J., Inaba, K., Garrett, W.S., et al., 2000. Transport of peptide- MHC class II complexes in developing dendritic cells. Science 288, 522–527.
Van Acker, H.H., Capsomidis, A., Smits, E.L., Van Tendeloo, V.F., 2017. CD56 in the immune system: more than a marker for cytotoxicity? Front. Immunol. 8, 892.
Van Haarst, J.M.W., Hoogsteden, H.C., de Wit, H.J., Verhoeven, G.T., Havenith, C.E.G., Drexhage, H.A., 1994. Dendritic cells and their precursors isolated from human bronchoalveolar lavage: immunocytologic and functional properties. Am. J. Respir. Cell Mol. Biol. 11, 344–350.
van Rijt, L.S., Prins, J.B., Leenen, P.J., Thielemans, K., de Vries, V.C., Hoogsteden, H.C., Lambrecht, B.N., 2002. Allergen-induced accumulation of airway dendritic cells is supported by an increase in CD31(hi)Ly-6C(neg) bone marrow precursors in a mouse model of asthma. Blood 100, 3663–3671.
West, M.A., Lucocq, J.M., Watts, C., 1994. Antigen processing and class II MHC peptide-loading compartments in human B-lymphoblastoid cells. Nature 369, 147–151.